Al-Rafidain Journal of Engineering Sciences
Journal homepage https://rjes.iq/index.php/rjes
ISSN 3005-3153 (Online)

A Numerical Studying Centrifugal Pumps Performance Using Non-Newtonian Fluids

Hawraa S. Sabty[1] and Hussam A. Khalaf[2]

[1,2] Department of Mechanical Engineering, College of Engineering, University of Thi-Qar, Thi-Qar 64001, Iraq.

ARTICLE INFO

Article history:
Received 24 July 2025
Revised 25 July 2025
Accepted 02 August 2025
Available online 02 August 2025

Keywords:

Shear-thickening Non-Newtonian fluids,
Centrifugal pump,
Viscosity,
Computational fluid dynamics (CFD),
Flow analysis.

ABSTRACT

This study presents a numerical analysis of mechanical pumps' function when working with Fluids that are not Newtonian. The complex rheological properties not Newtonian fluids, which are different from Newtonian fluids, have a significant influence on pump performance. Shear-thinning and shear-thickening properties are among these attributes. Using computational fluid dynamics (CFD) simulations, key performance parameters like head, efficiency, and power consumption were investigated under different flow conditions. The results demonstrate how fluid rheology affects internal flow patterns, pressure distribution, and overall pump efficiency. This study provides useful information about how to optimize centrifugal pump designs for industries that deal with non-Newtonian fluids, such as chemical manufacturing, food processing, and pharmaceuticals. The non-Newtonian fluids harm on the properties of an engineered centrifugal pump to pump water 40 l/min and 3300 rpm. in terms of numbers. A number The investigation was conducted using the Computational Fluid Dynamics technique. The analyses were conducted using water and three distinct non-Newtonian fluids generated from Carboxy Methyl Cellulose (CMC) solution: CMCs of 0.4%, 0.3%, and 0.2%. The assessments seemed conducted using rotor speeds of 3300 rpm and 1400 rpm with flow rates between 10 and 80 liters per minute. According to the findings, the pump performed better 3300 rpm with non-Newtonian fluids as opposed to water as contrasted as high as 1400 rpm.

1. Introduction

Centrifugal pumps are crucial to numerous sectors, such as wastewater treatment, chemical processing, and the manufacturing of food and pharmaceuticals. These pumps are renowned for their efficiency, robust

Corresponding author E-mail address: hussam.khalaf@utq.edu.iq
https://doi.org/10.61268/691qd484

design, and versatility in handling a range of fluids[1]. Despite their proven efficacy with Newtonian fluids—which are characterized by a constant viscosity irrespective of shear rate—pushing nonNewtonian fluids poses significant challenges. Non-Newtonian fluids, such as slurries, polymer solutions, and biological materials, display complex rheological phenomena, such as shearthinning, shear-thickening, and viscoelasticity[2]. Pump performance may be significantly impacted by these actions. Non-Newtonian fluids differ significantly from Newtonian fluids in that their behavior is determined by their varied viscosity under various flow conditions[3]. Unusual pressure distributions, flow patterns, and energy losses are caused by this variance in the pump. For instance, as the shear rate rises, shear-thinning fluids become less viscous, reducing hydraulic losses; conversely, shear-thickening fluids have the opposite effect, potentially requiring more energy[4]. Additionally, the viscoelastic characteristics of some non-Newtonian fluids can result in secondary flows and oscillations, which further complicates pump functioning. Due to these complexities, understanding the interplay between centrifugal pump dynamics and nonNewtonian fluid properties is essential for optimizing pump design and ensuring efficient operation[5]. In particular, fluid dynamics computation (CFD) has developed into a powerful tool for comprehending these interactions. Through the use of CFD models, researchers may investigate intricate flow phenomena such as velocity profiles, pressure gradients, and turbulence features without fully relying on costly and time-consuming experimental testing[6].

The effectiveness of these pumps when dealing with non-Newtonian fluids is examined statistically in this paper. Key performance indicators such as head, efficiency, flow rate, and power consumption will be investigated in order to quantify the specific effects of fluid rheology[7]. The findings are meant to advance our understanding of non-Newtonian fluid behavior in centrifugal pumps and provide recommendations for improving pump performance and design in industries where these fluids are often used. Numerical evaluations of water and non-Newtonian fluids, including CMCs of 0.2%, 0.3%, and 0.4%, were conducted at rotor speeds of 3300 rpm and 1400 rpm and flow rates between 10 and 80 l/min.

2. Method and approach

The M 10 x 12 HD Gardner Denver (GD) pump simulation was used for this investigation (Fig.1). The fluid exit is at a right angle to the working fluid inlet, which is located in the middle of the impeller (the rotating component). the stationary portion of the pump shaft at the volume, this model depicts a radial flow pump. Nonetheless, the ESP systems are said to be coupled with these centrifugal pumps [37].

On this particular instance investigation, a radial centrifugal water pump of the closed type that was intended to run at 3300 rpm and 40 l/min was employed. It was found that the pump impeller's diameter was 50 mm. The impeller with six blades and an outlet blade angle of was depicted in three dimensions in Figure 2.[8]

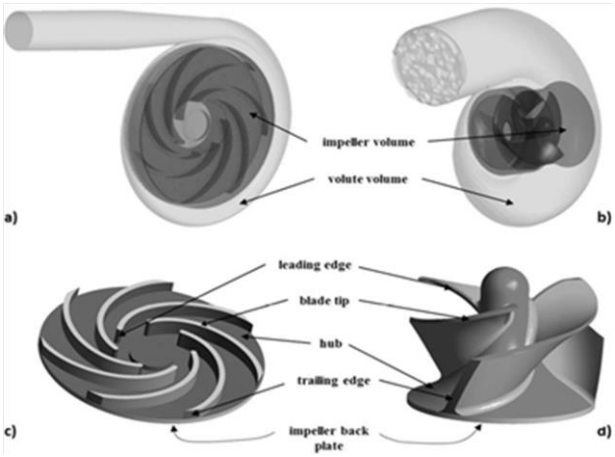

Figure 1 Reference names for pump components include: a) Pump 1 volume names, b) Pump 2 volume names, c) Pump 1 surface names, and d) Pump 2 surface names.

Table 1 provides a summary of the researched pump's design parameters. [1].

Impeller characteristics	
Flow rate	0.67 kg/sec
Head	40m
speed of rotation	1400 RPM
Efficiency	0.67
Inlet diameter	400mm
Outlet diameter	80
Hub diameter	21
Inlet angle	15
Outlet angle	14
Blade thickness	13mm
Blade number	4,5,6,7,8
Outlet width	62mm
Volute specifications	
Inlet width	115mm
Cutwater clearance	24mm
Cutwater thickness	9mm
Exit hydrodynamic diameter	216mm

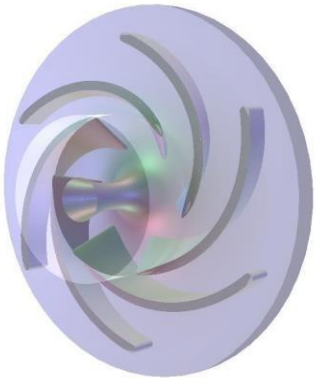

Figure 2: Three-dimensional impeller visualization

The machine that pumps was designed using CFX and CFD software. The centrifugal pump impeller employed turbo grid mesh, which may resolve complex impeller blade issues. Figure 3 (a) and (b) depict the centrifugal pump's turbo grid mesh impeller and the unstructured mesh of the pump's volute, respectively. A fine mesh with 1401968 total elements and 1358265 total nodes was supplied.[9]

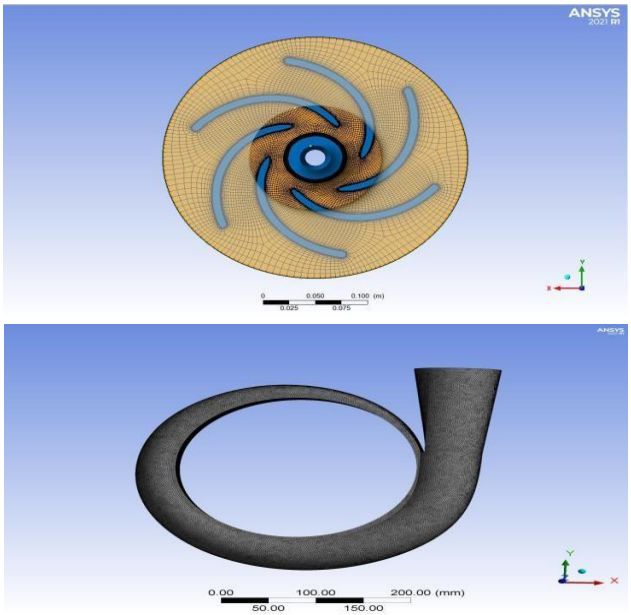

Figure 3 shows the (a) grid-structured turbo impeller mesh and the (b) unstructured volute mesh.

Numerous researchers employed a variety of turbulence models in their numerical assessments of the centrifugal pump. In their numerical analysis RNG k-ε turbulence, k-ε, and k-ω were employed by Kaewnai et al[9]. models. discovered that the differences amongst turbulence models were only 0.3%. They selected turbulence densities of 1%, 5%, and 10%, and for each turbulence intensity, the same head effect was seen. The analyses in this work were conducted using a 5% turbulence intensity Considering the model of k-ε turbulence.

The momentum equations can be expressed as follows, and The

incompressible and unstable continuity served as the governing equations[8]:

$$\frac{\partial \rho}{\partial t} + \bar{\nabla}.\rho\bar{V} = 0 \quad (1)$$

$$\rho\frac{d\bar{V}}{dt} + \bar{\nabla}P = \rho\bar{g} + \mu(\nabla^2.\bar{V}) - 2\rho\bar{\Omega}\times\bar{V} - \rho\bar{\Omega}\times(\bar{\Omega}\times\bar{r}) \quad (2)$$

Transport equations for k and ε in the standart k- ε model are defined as:

$$\frac{\partial(\rho k)}{\partial t} + \nabla.(\rho k u) = \nabla\left[\frac{\mu_k}{\sigma_k}\nabla_k\right] + 2\mu_k(E_{ij}.E_{ij}) - \rho\varepsilon \quad (3)$$

$$\frac{\partial(\rho\varepsilon)}{\partial t} + \nabla(\rho\varepsilon u) = \nabla\left[\frac{\mu_t}{\sigma_\varepsilon}\nabla_\varepsilon\right] + \mathrm{C}_{1\varepsilon}\frac{\varepsilon}{k}2\mu_t(E_{ij}.E_{ij}) - \mathrm{C}_{2\varepsilon}\rho\frac{\varepsilon^2}{k} \quad (4)$$

The total of the turbulent vortex viscosity and the molecular viscosity is known as the effective viscosity. Where is $\mu_t = \rho\mathrm{C}_\mu L_t\sqrt{k}$ k . In the viscosity of the unstable vortex, C_μ which is a scale of length, L_t is a m which is a scale of length An equation mathematical connection exists that is $\varepsilon = \sqrt{k^3}/L_t$ between L_t and the rate of turbulence. In the equations of transport for k and ε , $\mathrm{C}_{1\varepsilon}$, C_μ , C_k $C_{2\varepsilon}$ and σ_ε A scale of length is a swirling vortex, which is a constant. A which is a scale of length are constants. These Variables within the conventional k-ε Designs are C_μ = 0.09 , C_k = 1.00, $\mathrm{C}_{1\varepsilon}$ = 1.44 , $\mathrm{C}_{2\varepsilon}$ = 1.92 and σ_ε = 1.30. E_{ij} displays the average rate of deformation over time.

Its tensor. As seen in Fig. 4, numerical analyses were conducted using four to eight blades. The centrifugal pump contains four (a), six (b), and eight (c) blades, and 50 mm is the impeller's exit diameter. The angle of the exit blade is 22.50°.

Figure 4: Shows impellers with varying numbers of blades: (a) blade number four, (b) blade number six, and (c) blade number eight.

The numerical analysis's efficiency values in the water-based analysis with different numbers of blades are displayed in Table 1. The number 4 blades had an extreme loss of circulation, while the number 8 blades' high surface friction resistance and significant flow obstruction resulted in larger impeller losses. The ideal number of blades was discovered to be six since the 6-blade impeller had the maximum efficiency. The goal of the analysis was to find the centrifugal pump impeller's ideal

outlet blade angle with six blades. The maximum efficiency point was determined to be. The outlet blade angle was selected between. Thus, by improving the pump head, it increased by around 2 percent. the angle of the output blade.

Table 1: The efficiency according to the various blade counts.

Parameters	Efficiency (%)
Blade no:4	67.2
Blade no:5	67.80
Blade no:6	68.70
Blade no:7	68.29
Blade no:8	67.72

The centrifugal pump's closed-type impeller was designed using a rotating frame of reference technique. The impeller's rotational speed was operated between 1400 and 3300 rpm. A total pressure of 1 atm and a five percent turbulence intensity were used as the boundary condition at the inlet. For every solid surface, A condition of mass flow rate was selected at the outflow and the no-slip wall boundary requirement was implemented. Behavior of the non-Newtonian fluid was described using power law, and the k-ε turbulence model was selected One definition of shear stress is $= k\gamma^n$

Fluids that are not Newtonian and water with The CMC values of 0.4%, 0.3%, and 0.2% that behave rheologically similarly to oil were the subjects of numerical analyses. Table 2 lists The strength law's parameters K and n for CMCS 0.4%, 0.3%, and 0.2% [10].

Table 2 Pinho and Whitelaw's analysis of non-Newtonian fluid flow within a conduit yielded the K and n are power law parameters.

Solution	**K(pa.s)**	**N**
CMC, which is 0.4%	0.447	0.56
CMC, which is 0.3%	0.184	0.64
CMC, which is 0.2%	0.044	0.75

5. Results and Discussions

The impacts of flow rates and rotor speed were examined numerically in order to examine non-Newtonian fluids of CMC 0.3%, 0.4%, 0.5%, and CMC 0.2% and their centrifugal pump characteristics and CMC 0.1%. The water values were compared to all of the results. Fig. 5(a) and (b) show the pump's Distributions of

pressure and velocity for CMC %0.2 at Q=40 l/min, respectively.

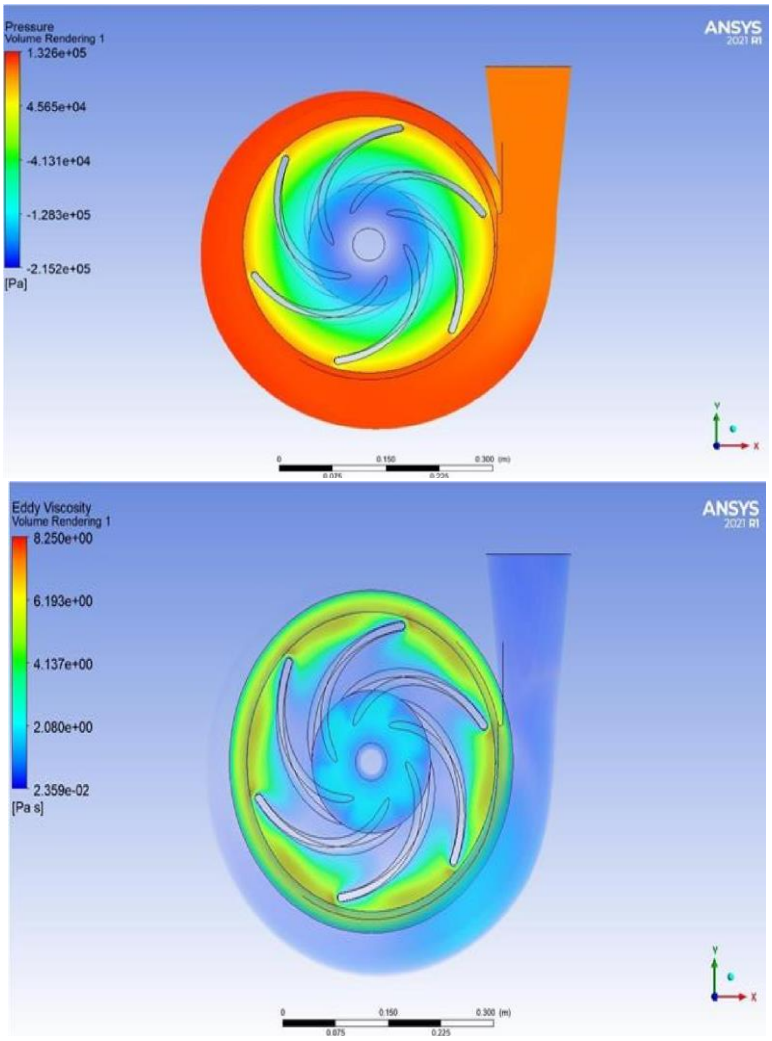

Figure 5 Shows the CMC percentage at Q=40 l/min, 0.2,

along with the distributions of speed and pressure.

Pressure mounted from the front-runner edge of the impeller to the trailing edge because of the dynamic head that the pump's rotating impeller produces.as it descends toward the volute's outlet. The impeller's discharge achieved the centrifugal pump's maximum pressure of 1.51 atm. The pump impeller's velocity rose as it neared the impeller, reaching its maximum of 9.62 m/s. Figure 6 displayed the head variation with all fluid flow rates at 3300 rpm. For all fluids, the head dropped as the flow rate increased. The CMC concentrations' pump head rise was marginally greater than the water's value (b) As volumetric pressure increased, compared to CMC 0.3% and CMC 0.2%, the pump head for CMC 0.4% deterioration was greater.

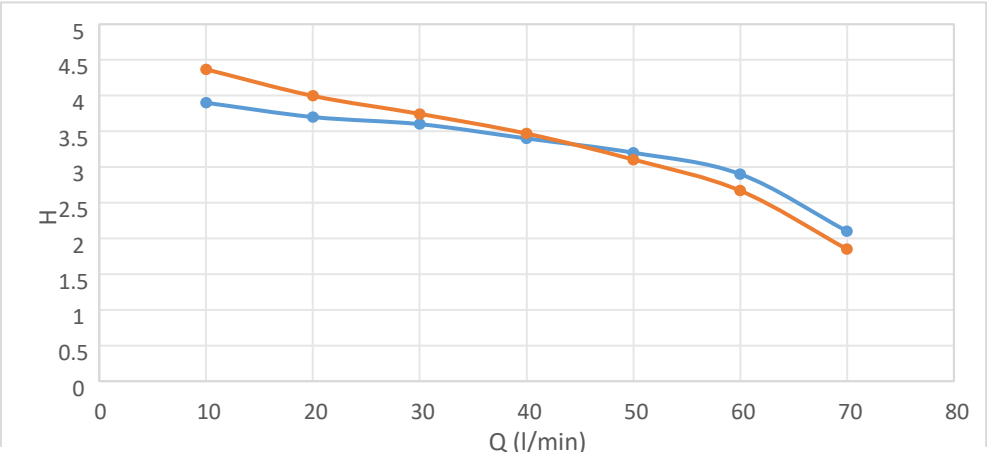

Figure 6 Head changes at 3300 rpm with flow rates.

Figure 7 shows the changes in head with flow rates at 1400 rpm. Similar to 3300 rpm, When the rate of flow increased, the pump head decreased. The pump's centrifugal maximum head increase was recorded at 1400 0.8 H(m) 0.6 0.4 0.2 0 40 60 Q(l/min) 80 rpm for water and 3300 rpm for CMC 0.2%. CMC 0.4% had the lowest value at 1400 rpm. At rotor speeds of 3300 rpm and flow rates of 20 l/min, the pump head was 3.7880 m for CMC 0.2% and 3.7028 m for water. The head at 20 l/min and 1400 rpm for water and CMC 0.2% was also found to be 0.6204 m and 0.6195 m, respectively.

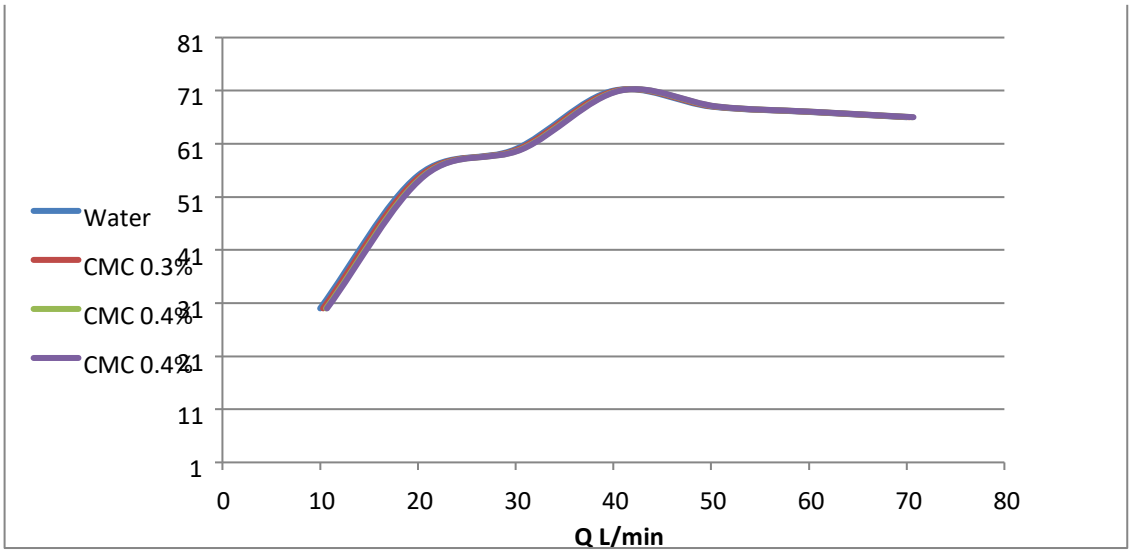

Figure 7 Head fluctuation at 1400 rpm with flow rates

The fluids' Q-η curve at 3300 rpm was shown in Fig. 8. Approximately 40 l/min flow rates, or the pump's BEP 3300 revolutions per minute, yielded highest effectiveness Most of all fluids. At BEP, efficiency values for 40 CMC 0.2% and water were found to be 68.851% and 68.7134%, respectively. At BEP, there was a difference of roughly 0.2% between CMC 0.2% and water, and a difference of roughly 2% between CMC 0.4% and water.

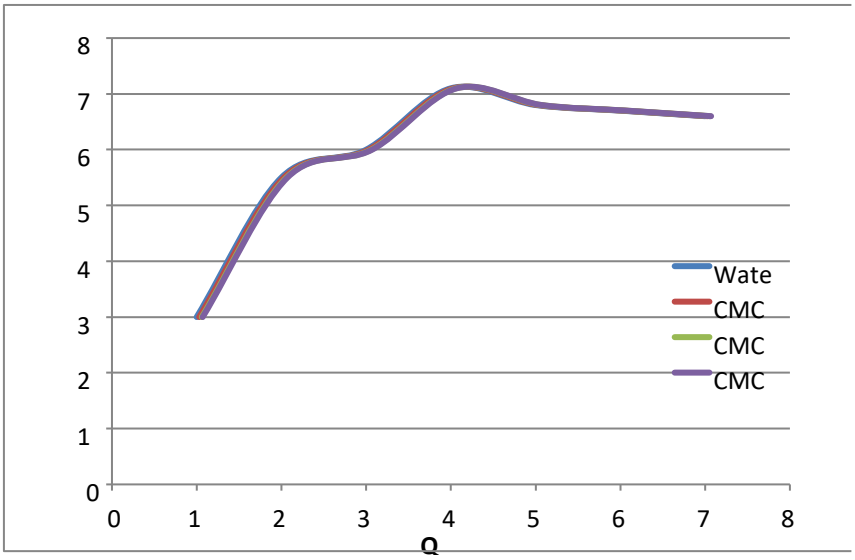

Figure 8: Efficiency changes with flow rate at 3300 rpm.

Fig. 9 displayed the efficiency fluctuation at 1400 rpm changing a high flow rate. All fluids reached their optimum efficiency at around 20 l/min, or At 3300 rpm, 40 l/min. The water efficiency metrics exceeded the concentrations of carboxymethyl cellulose at 1400 rpm. The CMC 0.2% efficiency for 20 l/min was 80 η(%) 60 40 20 0 67.0506% and 51.827%, respectively, at 1400 and 3300 rpm, while the water value was 67.8863% and 52.1662% at those speeds. Furthermore, the CMC 0.4% efficiency value was determined to be 65.7778% between 1400 and 3300 rpm. 53.7213%, in that order

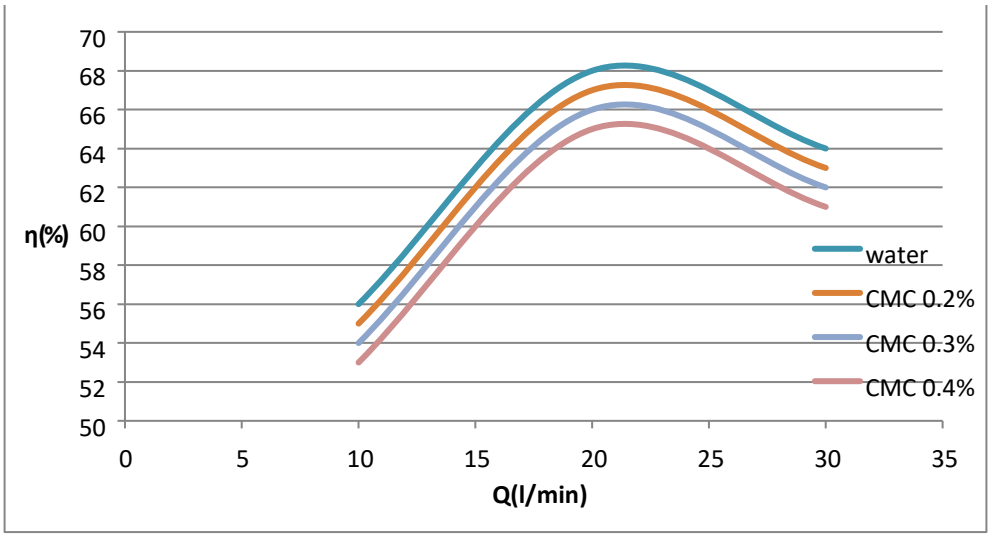

Figure 9 The variation of the head with flow rates at 3300 rpm

The CMC %0.2 viscosity values the between 1400 and 3300 rpm 53.7213%, in that order efficiency points are displayed with Figure 10 , in that order. The values of viscosity at the following edge of blades were higher than those near superiority in both rotor speeds. Additionally, the viscosity of 40 Q(l/min) peaked close to the volute tongue and then rose toward the volute's outflow. The

maximum and average viscosity values were higher at 1400 rpm than 3300 rotations per minute.

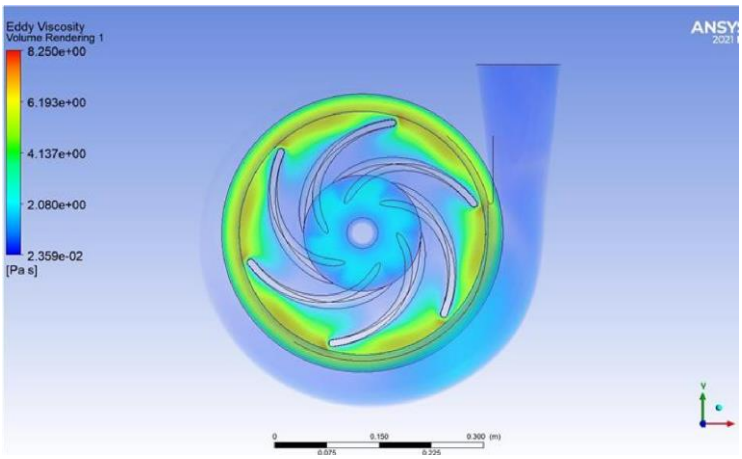

Figure 10 The amounts of CMC %0.2 viscosity at 1400 rpm and 40 l/min.

6. Conclusions

This study included a numerical analysis of the centrifugal pump's performance parameters with fluids from water, Rotor CMCs of 0.4%, 0.3%, and 0.2% speed values between 3300 and 1400 rpm, with flow rates between 10 and 80 l/min. The water centrifugal pump's head and efficiency were increased by optimizing The amount of blades and output angle of the blade. The BEP was measured at approximately 40 l/min, 20 l/min flow rates between 3300 and 1400 rpm, respectively, for every fluid. The head rise of the pump utilizing carboxymethyl cellulose solutions was found to be somewhat 1400 rpm, below the sea., in in contrast to the data With the same flow rate at 3300 rpm with a fast The rotating part. At design specifications, centrifugal pump's performance characteristics showed their peak at CMC 0.2%.

References

[1] G. Zhang, M. Zhang, W. Yang, X. Zhu, and Q. Hu, "Effects of non-Newtonian fluid on centrifugal blood pump performance," *Int. Commun. Heat Mass Transf.*, vol. 35, no. 5, pp. 613–617, 2008, doi: 10.1016/j.icheatmasstransfer.2007.11.005.

[2] E. C. Bacharoudis, A. E. Filios, M. D. Mentzos, and D. P. Margaris, "Parametric Study of a Centrifugal Pump Impeller by Varying the Outlet Blade Angle," *Open Mech. Eng. J.*, vol. 2, no. 1, pp. 75–83, 2008, doi: 10.2174/1874155x00802010075.

[3] M. H. Shojaeefard, M. Tahani, M. B. Ehghaghi, M. A. Fallahian, and M. Beglari, "Numerical study of the effects of some geometric characteristics of a centrifugal pump impeller that pumps a viscous fluid," *Comput. Fluids*, vol. 60, pp. 61–70, 2012, doi: 10.1016/j.compfluid.2012.02.028.

[4] B. R. Chakraborty, Sujoy KM Pandey, "Numerical Analysis on Effects of Blade Number Variations on Performance of Centrifugal Pumps with Various Rotational Speeds," *Int. J. Energy Power Eng.*, no. 2002, p. 10, 2012, [Online]. Available: http://inpressco.com/category/ijcet

[5] Y. Li, Z. Zhu, Z. He, and W. He, "Abrasion characteristic analyses of solid-liquid two-phase centrifugal pump," *J. Therm. Sci.*, vol. 20, no. 3, pp. 283–287, 2011, doi: 10.1007/s11630-011-0471-8.

[6] N. Aldi *et al.*, "Experimental and Numerical Analysis of a Non-Newtonian Fluids Processing Pump," *Energy Procedia*, vol. 126, pp. 762–769, 2017, doi: 10.1016/j.egypro.2017.08.247.

[7] S. Abazariyan, R. Rafee, and S. Derakhshan, "Experimental study of viscosity effects on a pump as turbine performance," *Renew. Energy*, vol. 127, pp. 539–547, 2018, doi: 10.1016/j.renene.2018.04.084.

[8] M. Donmez and O. Yemenici, "A Numerical Study on Centrifugal Pump Performance with the Influence of Non-Newtonian Fluids," *Int. J. Sci.*, vol. 8, no. 04, pp. 39–45, 2019, doi: 10.18483/ijsci.2010.

[9] S. Kaewnai, M. Chamaoot, and S. Wongwises, "Predicting performance of radial flow type impeller of centrifugal pump using CFD," *J. Mech. Sci. Technol.*, vol. 23, no. 6, pp. 1620–1627, 2009, doi: 10.1007/s12206-008-1106-1.

[10] N. F. Mechanics, E. S. P. B. V, F. T. Pinho, J. H. Whitelaw, F. Section, and E. Road, "129 flow of non-newtonian fluids in a pipe," vol. 34, pp. 129–144, 1990.